Advection and the Efficiency of Spectral Energy Transfer in Two-Dimensional Turbulence

Lei Fang and Nicholas T. Ouellette

Phys. Rev. Lett. **117**, 104501 — Published 30 August 2016

DOI: 10.1103/PhysRevLett.117.104501

Advection and the Efficiency of Spectral Energy Transfer in Two-Dimensional Turbulence

Lei Fang and Nicholas T. Ouellette*
Department of Civil and Environmental Engineering, Stanford University, Stanford, California 94305, USA

We report measurements of the geometric alignment of the small-scale turbulent stress and the large-scale rate of strain that together lead to the net flux of energy from small scales to large scales in two-dimensional turbulence. We find that the instantaneous alignment between these two tensors is weak, and thus that the spectral transport of energy is inefficient. We show, however, that the strain rate is much better aligned with the stress at times in the past, suggesting that the differential advection of the two is responsible for the inefficient spectral transfer. We provide evidence for this conjecture by measuring the alignment statistics conditioned on weakly changing stress history. Our results give new insight into the relationship between scale-to-scale energy transfer, geometric alignment, and advection in turbulent flows.

The primary feature that distinguishes turbulence from more generic unsteady flow is the directed flux of energy from the scales at which it is injected into the flow to the scales at which it is dissipated [1]. This flux proceeds from large to small scales in three dimensions in a "direct" cascade, and in an "inverse" cascade from small to large scales in two dimensions. Although the intricate details are not fully understood, there is general consensus on the broad mechanisms that drive these cascades. Building on ideas going back to Taylor [2, 3], the 3D direct cascade is thought to be the consequence of the stretching, and therefore intensification, of vortices by the turbulent strain [4]. In 2D, vortex stretching cannot occur for geometric reasons; instead, a vortex thinning mechanism, where patches of (conserved) vorticity are reoriented and distorted by the turbulent strain without changing their circulation, is taken to be responsible for the inverse transfer of energy from small to large scales [5, 6].

As with any energy flux, turbulent cascades can be interpreted as the result of the action of a stress against a rate of strain. In turbulence, the requisite stress arises from the exchange of momentum between scales due to the nonlinearity in the Navier–Stokes equations. In 3D, the large scales do work on the small scales, transferring energy to them; and in 2D, the small scales do work on the large scales. Once cast in this language, it becomes clear that the relative geometry of the turbulent stress and the large-scale strain rate is key to determining the efficiency of the energy cascade: components of the turbulent stress that are orthogonal to the strain rate can do no work, and therefore cannot transfer any energy. Thus, one would expect strong alignment between these two tensors to explain the observation that all turbulent flows display a cascade. In both 2D and 3D turbulence, however, it has long been known that the alignment is surprisingly weak [7]. In 3D, with some assumptions [8], one can relate the stress–strain-rate alignment to the alignment between the vorticity vector and the eigenvectors of the strain rate. Efficient downscale transfer of energy requires that the vorticity be aligned with the most extensional eigenvector of the strain rate; however, vorticity is well known to align instantaneously with the *intermediate* strain-rate eigenvector instead [9]. Although this intermediate eigenvector is also weakly extensional in turbulence [9], the misalignment with the most strongly stretching direction would appear to severely limit the amount of energy that can be driven downscale in the cascade. Likewise, in 2D, the stress and strain rate are on average nearly perfectly misaligned [10, 11], again leading to an energy flux that is much weaker than it might otherwise be.

It has recently been argued that in 3D turbulence, this conundrum can be resolved by properly accounting for advection [12–14]: by noting that both vorticity and strain evolve spatiotemporally, it has been shown that the apparent alignment of vorticity with the intermediate strain-rate eigenvector occurs because the vorticity is in fact aligned preferentially with the direction of the extensional eigenvector at a previous time. In this Letter, we show that a similar effect occurs in 2D turbulence. Using a filter-space technique to study the flux of energy between scales in a spatially resolved way [10, 15–21], we measure both the turbulent stress and the large-scale strain rate. By considering the inner product of these two tensors measured at different times along Lagrangian trajectories, we show that the degree of alignment varies with the time lag; in particular, we find that the (large-scale) strain rate lags the (small-scale) stress. Thus, we find that the strain rate attempts to align with the *previous* direction of the stress, much as was observed for strain and vorticity in 3D turbulence [12, 13]. To confirm this interpretation, we consider the conditional statistics of the alignment for trajectories along which the stress exhibited little change; consistently, these cases show a higher degree of alignment than the full ensemble of trajectories does. Our results lead to the conclusion that advection tends to disrupt the delicate geometric balance that is required to transfer energy from scale to scale, thereby reducing the efficiency of the turbulent cascade.

To study this alignment, we conducted experiments in an electromagnetically driven thin-layer flow cell that produces nearly two-dimensional flow [22]. We have described this apparatus in detail previously [20, 22], and so we do so only briefly here. The working fluid is a uniform layer of salt water (16% NaCl by mass in deionized water) measuring $86 \times 86 \times 0.5$ cm^3. This fluid sits on a glass substrate above a square grid of neodymium-iron-boron permanent magnets spaced by $L_m = 25.4$ mm. The magnetic poles point vertically, and are arranged in stripes of alternating polarity. By passing a d.c. electric current laterally through the fluid, we can apply a Lorentz body force and generate flow. As long as the current is not too large, this arrangement produces a nearly 2D flow field [22]. The nondimensional strength of the forcing can be captured by the in-plane Reynolds number $\mathrm{Re} = u' L_m/\nu$, where u' is the root-mean-square velocity and ν is the kinematic viscosity [23]. Here, $\mathrm{Re} = 270$. To measure the flow field, we use particle tracking velocimetry. We seed the flow with 51-μm-diameter fluorescent polystyrene microspheres. To remove any clustering effects due to surface tension and to confine the particles to a single plane, we float a layer (also 5 mm deep) of less-dense pure water on top of the salt-water layer; the particles lie on the (miscible) interface between the two. We image the motion of the particles from above with a 4-megapixel camera at 60 frames per second. We extract particle trajectories from the movies using a multi-frame predictive tracking algorithm [24], from which accurate velocities can be calculated. Since we track roughly 30,000 particles per frame, they are spatially dense enough that highly resolved Eulerian velocity fields can be determined; to do so while also removing noise and ensuring two-dimensionality, we project the measured particle velocities onto a basis of streamfunction eigenmodes [22]. Subsequently, to compute accurate and unbiased Lagrangian statistics with desired initial conditions, we construct virtual fluid-element trajectories by integrating their kinematic equations of motion [25].

Studying the details of the flux of energy between scales in turbulence has historically been challenging. Spectral methods can provide the mean transfer of energy, but after Fourier transforming, all connection to the spatial degrees of freedom of the flow is lost. Here, we instead use a filter-space technique (FST) to resolve the energetic coupling between scales simultaneously in space and in scale [10, 16–21]. The core of an FST is the application of a spectral low-pass filter to the measured velocity field. If this filter has a cutoff lengthscale of r, then all variation of the field on scales smaller than r is suppressed, while the large-scale structure is retained. The utility of this approach becomes clear when one considers, for example, the equation of motion for the filtered kinetic energy $E^{(r)} = (1/2)u_i^{(r)}u_i^{(r)}$, where the superscript (r) denotes the cutoff scale of the filter and summation is implied over repeated indices. The most salient difference between this equation and that for the full kinetic energy is the appearance of the new term

$$\Pi^{(r)} = -\left[(u_i u_j)^{(r)} - u_i^{(r)} u_j^{(r)}\right] \frac{\partial u_i^{(r)}}{\partial x_j} = -\tau_{ij}^{(r)} s_{ij}^{(r)}, \quad (1)$$

where $s_{ij}^{(r)}$ is the rate of strain (that is, the symmetric part of the velocity gradient) of the filtered velocity field and $\tau_{ij}^{(r)}$ is a turbulent stress tensor. $\Pi^{(r)}$ can be interpreted as the flux of energy between scales smaller than r and scales larger than r; for more details and a full derivation of this term, see Refs. [17, 18, 20]. And unlike in a fully spectral approach, $\Pi^{(r)}$ can be measured at any spatial location, since it only depends on spatially local quantities. With our sign convention, $\Pi^{(r)} < 0$ denotes a flux of energy from small scales to large (i.e., inverse energy flux), while $\Pi^{(r)} > 0$ denotes a flux of energy from large scales to small.

In 2D, $\Pi^{(r)}$ can be re-expressed in terms of the largest eigenvalues $\lambda_\tau^{(r)}$ and $\lambda_s^{(r)}$ of the (deviatoric) stress and strain rate, respectively, and the angle $\Theta_{s\tau}^{(r)}$ between the corresponding (unit) eigenvectors $\hat{\mathbf{e}}_\tau^{(r)}$ and $\hat{\mathbf{e}}_s^{(r)}$ as [11, 21, 26]

$$\Pi^{(r)} = -2\lambda_\tau^{(r)}\lambda_s^{(r)} \cos 2\Theta_{s\tau}^{(r)}. \quad (2)$$

Written in this way, it is clear that the alignment of the stress and the strain rate is critical for determining the local energy flux between scales. In particular, when the eigenframes of the stress and the strain rate are oriented at 45° with respect to each other, the energy flux will vanish regardless of the magnitudes of these tensors; and indeed, as we have shown previously [11], $\Theta_{s\tau}^{(r)}$ is more highly correlated with the spatial structure of $\Pi^{(r)}$ than are $\lambda_\tau^{(r)}$ or $\lambda_s^{(r)}$. Thus, we suggest here that $|\cos 2\Theta_{s\tau}^{(r)}|$ can be thought of as the efficiency of the energy transfer mechanism, as it directly gives the fraction of the turbulent stress that does work against the large-scale strain and therefore transfers energy between scales. When $\Theta_{s\tau}^{(r)} = 0$, the stress and the strain rate are perfectly aligned and this efficiency goes to unity; when $\Theta_{s\tau}^{(r)} = 45°$, they are perfectly misaligned and the efficiency vanishes. When $\Theta_{s\tau}^{(r)} = 90°$, the stress aligns perfectly with the *compressive* strain-rate eigenvector, giving again a maximally efficient energy transfer but toward smaller length scales.

In Fig. 1, we show the mean (averaged over space and time) values of $\Pi^{(r)}$ and $\Theta_{s\tau}^{(r)}$ as functions of the filter scale r. These results are relatively insensitive to the particular implementation of the FST [18]; here, we used a spatially isotropic finite impulse response filter constructed by convolving a sharp spectral filter with a frequency cutoff of $2\pi/r$ with a Gaussian window function that reduces ringing. As we have observed before

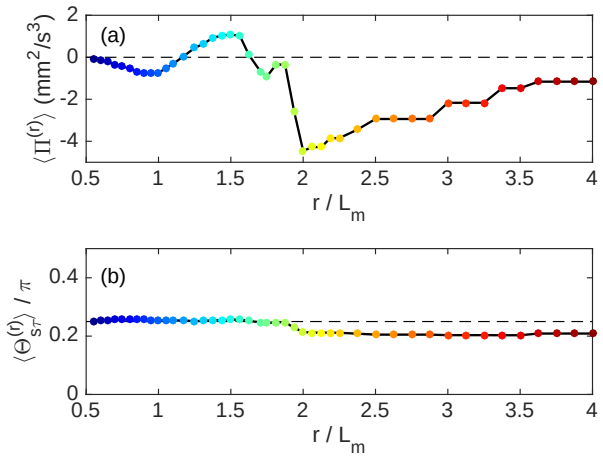

FIG. 1. (a) Mean spectral energy flux $\Pi^{(r)}$ as a function of the filter scale r scaled by the magnet spacing L_m. Negative values correspond to a flux of energy to larger length scales. (b) Mean instantaneous angle $\Theta^{(r)}_{s\tau}$ (in units of π) between the eigenframes of the stress $\tau^{(r)}_{ij}$ and the strain rate $s^{(r)}_{ij}$ as a function of filter scale r. The dashed line shows 45°.

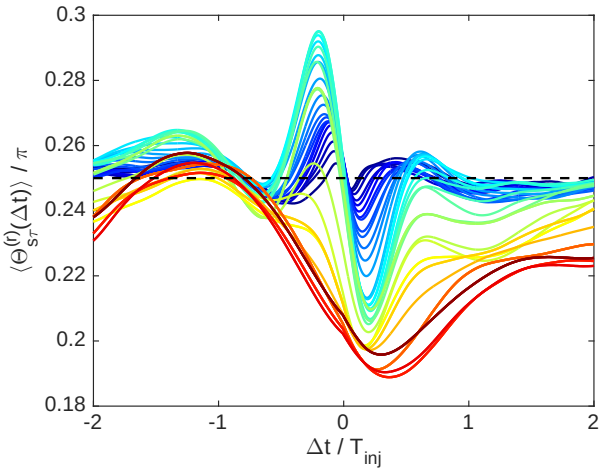

FIG. 2. Average of $\Theta^{(r)}_{s\tau}(\Delta t)\rangle$, the angle between the eigenframes of the stress at one time and the strain rate at a time Δt later, for several different filter scales r. Each curve shows $\Theta^{(r)}_{s\tau}(\Delta t)\rangle$ for a different r, and the colors correspond to the colors of the symbols in Fig. 1. The dashed line shows 45°.

[11], for length scales above $\sim 1.6L_m$, which we take to be roughly the energy injection lengthscale $L_{\rm inj}$, we see net inverse energy flux, as is expected in two-dimensional turbulence, although without a developed inertial range given that our Reynolds number is relatively low. The mean value of $\langle \Theta^{(r)}_{s\tau} \rangle$ is very close to 45°, the angle at which the stress and the strain rate are perfectly misaligned, at all scales, though slightly smaller where there is net inverse energy transfer. This result underscores the well known fact that the net energy cascade in turbulence arises from a weak asymmetry between locally strong forward and inverse transfer events [10, 18, 20, 27]. In terms of our efficiency language, for $r < L_{\rm inj}$ the energy transfer is completely inefficient; but even for $r > L_{\rm inj}$, where the energy cascade does appear to operate, $\langle \Theta^{(r)}_{s\tau} \rangle \approx 37°$ and the efficiency is only about 27%. Thus, the observed net energy flux through the cascade is much weaker than it otherwise might be.

This result naturally leads to the question of why the cascade is so inefficient. Here, we propose at least a partial answer: that advection upsets the delicate balance between the turbulent stress and the large-scale strain rate that is required for energy transfer between scales. A common explanation for the inverse energy cascade in 2D turbulence is a vortex-thinning mechanism [5, 6]. This picture considers the evolution of a initially circular small-scale vortex embedded in a large-scale strain field. It argues that as the vortex is stretched along the extensional straining direction and thinned along the compressive direction, its net kinetic energy will decrease (since its circulation must remain constant due to Kelvin's theorem but the length of its perimeter will increase due to the straining) but its net velocity will become oriented along the straining direction, producing a tensile turbulent stress that reinforces the large-scale strain [10]. For this picture to be correct, however, the initial vortex must remain embedded in a coherent strain field long enough for the thinning to occur—and thus, the vortex-thinning picture implicitly ignores the effects of advection, or at best assumes that the strain field and the vortex will be advected in lockstep. This is highly unlikely to be the case; for example, in 3D turbulence, it has long been known that rotation has a significantly longer correlation time along trajectories than does strain [28, 29]. Thus, as a vortex in a real, evolving turbulent flow begins to distort and align with the local large-scale strain, the strain field itself will change, leading to a weaker-than-expected instantaneous alignment.

To test this idea, we considered not the instantaneous alignment between $\tau^{(r)}_{ij}$ and $s^{(r)}_{ij}$ but rather the alignment between these two tensors computed at different times along the same Lagrangian trajectory. In Fig. 2, we plot

$$\langle \Theta^{(r)}_{s\tau}(\Delta t) \rangle = \langle \cos^{-1}(\hat{\mathbf{e}}^{(r)}_{\tau}(t) \cdot \hat{\mathbf{e}}^{(r)}_{s}(t + \Delta t)) \rangle, \qquad (3)$$

where the average is taken over an ensemble of many trajectories beginning from different initial positions at different times, for a range of filter scales r. In all cases, we see that $\langle \Theta^{(r)}_{s\tau}(\Delta t) \rangle$ *decreases* as Δt increases from 0; that is, we observe that the alignment between the stress now and the rate of strain later (or equivalently the rate of strain now and the stress previously) is stronger than the instantaneous value. The trend is the opposite for negative Δt; for negative time lags, the angle quickly equilibrates to 45°, which we would expect if the orientation of the two tensors were uncorrelated. For filter

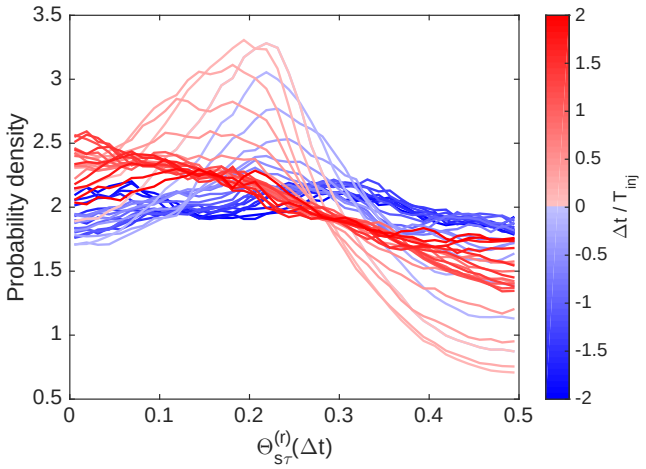

FIG. 3. Probability density functions (PDFs) of $\Theta^{(r)}_{s\tau}(\Delta t)\rangle$ at $r = 2L_m$ (the most intense inverse energy flux) for positive and negative Δt. For increasing positive Δt, the peak of the PDF shifts toward more alignment; however, for increasing negative Δt, the peak shifts toward misalignment and the PDF ultimately becomes uniform.

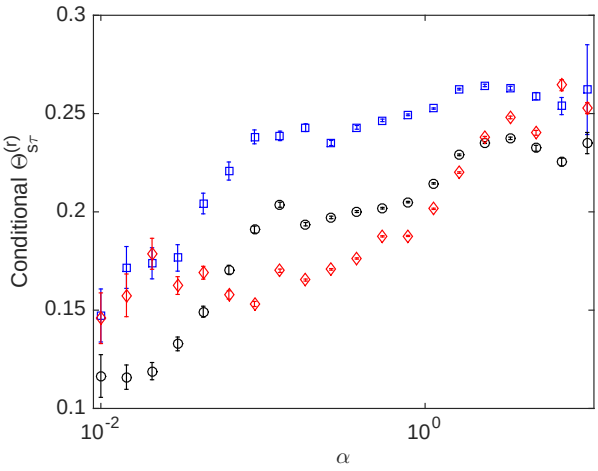

FIG. 4. Conditional averages of $\Theta^{(r)}_{s\tau}$ (see text for the definition) as a function of α, the multiplier of the ensemble-averaged stress-angle standard deviation. Smaller values of α correspond to less prior variation in the orientation of the stress eigenframe. Data are shown for three filter scales: $r = L_m$ (squares), $r = 2L_m$ (circles), and $r = 3L_m$. Error bars show the standard error of the mean. In all cases, weaker prior variability of the stress eigenframe orientation corresponds to stronger instantaneous alignment between the stress and the rate of strain.

scales smaller than L_{inj}, the increasing alignment we see for positive Δt quickly disappears, consistent with the expectation that any tendency toward a net cascade in this range of scales should be weak. For larger r, however, the net alignment persists for several injection timescales $T_{\text{inj}} = L_{\text{inj}}/u'$. These results allow us to draw two conclusions. First, it is clear that the alignment between the stress and the strain rate has coherent dynamics, and therefore that advection plays a role in disrupting the instantaneous alignment, just as it does in 3D turbulence [12–14]. And second, since the alignment is enhanced for positive Δt, our results indicate that the rate of strain follows the turbulent stress, in apparent contradiction to the standard vortex thinning picture [10].

This second conclusion can be bolstered by considering the full probability density functions (PDFs) of $\Theta^{(r)}_{s\tau}(\Delta t)$ in addition to just the mean value for different Δt, as we show in Fig. 3 for both positive and negative Δt. As Δt increases in forward time from 0, the peak of the PDF shifts to lower values, eventually hitting $\Theta^{(r)}_{s\tau}(\Delta t) \approx 0$ when $\Delta t \approx T_{\text{inj}}$. For negative time lags, however, the peak of the PDF shifts toward 45°, and the PDF eventually becomes uniform, indicating no preferred orientation between the current stress and the previous rate of strain.

Our measurements show that the orientation of the eigenframe of the large-scale rate of strain follows the evolution of the small-scale turbulent stress but with a time lag. We have argued that this result implicates the differential advection of the stress and the strain rate as the origin of the surprisingly weak instantaneous alignment of these two tensors. It then follows that if we consider only those trajectories for which the stress has not changed much in the past, we should expect to see stronger instantaneous alignment of the stress and the strain rate. To test this idea, we computed conditional statistics of $\Theta^{(r)}_{s\tau}$. To characterize the history of the stress along a trajectory, we first measured the time series of $\phi^{(r)}_\tau$, the angle between $\hat{\mathbf{e}}^{(r)}_\tau$ and the horizontal axis, for each trajectory. We take the standard deviation of $\phi^{(r)}_\tau$ over the previous T_{inj}, which we label $\sigma^{(r)}_\phi$, as a measure of the prior variability of the stress orientation. Instants along a trajectory for which $\sigma^{(r)}_\phi$ is small have experienced fairly uniform stress fields over their recent history. We then constructed the conditional averages $\left\langle \Theta^{(r)}_{s\tau} | \sigma^{(r)}_\phi = \alpha \langle \sigma^{(r)}_\phi \rangle \right\rangle$; that is, we measured the mean instantaneous $\Theta^{(r)}_{s\tau}$ given that the fluctuations of $\phi^{(r)}_\tau$ were some multiple α of the ensemble-averaged value. Our results for a range of α are shown in Fig. 4 for three different filter scales. In all cases, it is clear that, as conjectured, less prior variability in the orientation of $\tau^{(r)}_{ij}$ corresponds to stronger instantaneous alignment between the stress and the strain rate. Thus, our interpretation of our results is borne out by this conditional analysis.

We have demonstrated that the alignment between the turbulent stress and the large-scale rate of strain that is crucial for characterizing the efficiency of scale-to-scale energy transfer in turbulence cannot be understood without considering the effects of advection. In particular, our results show that the strain rate is better aligned

with the stress at previous times along Lagrangian trajectories that with its instantaneous value, implying that advection reduces the efficiency of the cascade from what it would be in a static turbulent field. These results argue that the typical vortex stretching and vortex thinning mechanisms thought to be responsible for the energy cascade may need to be modified to account for fluid motion properly.

This work was supported by the U.S. National Science Foundation under grants CBET-1600292 and CMMI-1563489.

* nto@stanford.edu

[1] G. Falkovich, "Symmetries of the turbulent state," J. Phys. A: Math. Theor. **42**, 123001 (2009).
[2] G. I. Taylor, "The transport of vorticity and heat through fluids in turbulent motion," Proc. R. Soc. Lond. A **135**, 685–702 (1932).
[3] G. I. Taylor, "Production and dissipation of vorticity in a turbulent fluid," Proc. R. Soc. Lond. A **164**, 15–23 (1938).
[4] H. Tennekes and J. L. Lumley, *A First Course in Turbulence* (MIT Press, Cambridge, MA, 1972).
[5] V. P. Starr, *Physics of Negative Viscosity Phenomena* (McGraw-Hill, New York, 1968).
[6] R. H. Kraichnan, "Eddy viscosity in two and three dimensions," J. Atmos. Sci. **33**, 1521–1536 (1976).
[7] J. M. Wallace, "Twenty years of experimental and direct numerical simulation access to the velocity gradient tensor: What have we learned about turublence?" Phys. Fluids **21**, 021301 (2009).
[8] V. Borue and S. A. Orszag, "Local energy flux and subgrid-scale statistics in three-dimensional turbulence," J. Fluid Mech. **366**, 1–31 (1998).
[9] W. T. Ashurst, A. R. Kerstein, R. M. Kerr, and C. H. Gibson, "Alignment of vorticity and scalar gradient with strain rate in simulated Navier-Stokes turbulence," Phys. Fluids **30**, 2343–2353 (1987).
[10] S. Chen, R. E. Ecke, G. L. Eyink, M. Rivera, M. Wan, and Z. Xiao, "Physical mechanism of the two-dimensional inverse energy cascade," Phys. Rev. Lett. **96**, 084502 (2006).
[11] Y. Liao and N. T. Ouellette, "Long-range ordering of turbulent stresses in two-dimensional flow," Phys. Rev. E **91**, 063004 (2015).
[12] H. Xu, A. Pumir, and E. Bodenschatz, "The pirouette effect in turbulent flows," Nat. Phys. **7**, 709–712 (2011).
[13] A. Pumir, E. Bodenschatz, and H. Xu, "Tetrahedron deformation and alignment of perceived vorticity and strain in a turbulent flow," Phys. Fluids **25**, 035101 (2013).
[14] R. Ni, N. T. Ouellette, and G. A. Voth, "Alignment of vorticity and rods with Lagrangian fluid stretching in turbulence," J. Fluid Mech. **743**, R3 (2014).
[15] M. Germano, "Turbulence: the filtering approach," J. Fluid Mech. **238**, 325–336 (1992).
[16] S. Liu, C. Meneveau, and J. Katz, "On the properties of similarity subgrid-scale models as deduced from measurements in a turbulent jet," J. Fluid Mech. **275**, 83–119 (1994).
[17] G. L. Eyink, "Local energy flux and the refined similarity hypothesis," J. Stat. Phys. **78**, 335–351 (1995).
[18] M. K. Rivera, W. B. Daniel, S. Y. Chen, and R. E. Ecke, "Energy and enstrophy transfer in decaying two-dimensional turbulence," Phys. Rev. Lett. **90**, 104502 (2003).
[19] D. H. Kelley and N. T. Ouellette, "Spatiotemporal persistence of spectral fluxes in two-dimensional weak turbulence," Phys. Fluids **23**, 115101 (2011).
[20] Y. Liao and N. T. Ouellette, "Spatial structure of spectral transport in two-dimensional flow," J. Fluid Mech. **725**, 281–298 (2013).
[21] Y. Liao and N. T. Ouellette, "Geometry of scale-to-scale energy and enstrophy transport in two-dimensional flow," Phys. Fluids **26**, 045103 (2014).
[22] D. H. Kelley and N. T. Ouellette, "Onset of three-dimensionality in electromagnetically forced thin-layer flows," Phys. Fluids **23**, 045103 (2011).
[23] D. H. Kelley and N. T. Ouellette, "Using particle tracking to meaure flow instabilities in an undergraduate laboratory experiment," Am. J. Phys. **79**, 267–273 (2011).
[24] N. T. Ouellette, H. Xu, and E. Bodenschatz, "A quantitative study of three-dimensional Lagrangian particle tracking algorithms," Exp. Fluids **40**, 301–313 (2006).
[25] N. T. Ouellette, P. J. J. O'Malley, and J. P. Gollub, "Transport of finite-sized particles in chaotic flow," Phys. Rev. Lett. **101**, 174504 (2008).
[26] Z. Xiao, M. Wan, S. Chen, and G. L. Eyink, "Physical mechanism the inverse energy cascade of two-dimensional turbulence: a numerical approach," J. Fluid Mech. **619**, 1–44 (2008).
[27] S. Chen, R. E. Ecke, G. L. Eyink, X. Wang, and Z. Xiao, "Physical mechanism of the two-dimensional enstrophy cascade," Phys. Rev. Lett. **91**, 214501 (2003).
[28] P. K. Yeung and S. B. Pope, "Lagrangian statistics from direct numerical simulations of isotropic turbulence," J. Fluid Mech. **207**, 531–586 (1989).
[29] S. S. Girimaji and S. B. Pope, "A diffusion model for velocity gradients in turbulence," Phys. Fluids A **2**, 242–256 (1990).